

Molecules with Perfect Cubic Symmetry as Nanobuilding Blocks for 3-D Assemblies. Elaboration of Octavinylsilsesquioxane. Unusual Luminescence Shifts May Indicate Extended Conjugation Involving the Silsesquioxane Core

S. Sulaiman,[†] A. Bhaskar,[†] J. Zhang,^{†,‡} R. Guda,[‡] T. Goodson III,^{†,‡} and Richard M. Laine^{*,†,§}

Departments of Materials Science and Engineering and Chemistry and the Macromolecular Science and Engineering Center, University of Michigan, Ann Arbor, Michigan 48109-2136

Received April 10, 2008. Revised Manuscript Received June 9, 2008

The objectives of this work are to demonstrate facile routes to 3-D star materials with octa- and hexadecafunctionality to provide new nanoconstruction tools for the synthesis of new types of stars, dendrimers, and hyperbranched molecules or for the assembly of novel nanocomposites. A further objective is to identify novel properties inherent in the resulting new compounds. Octavinylsilsesquioxane (OVS, [VinylSiO_{1.5}]₈) with perfect 3-D or cubic symmetry is elaborated through metathesis with substituted styrenes to produce a series of RStyrenylOS compounds. The *p*-BrStyrenylOS compound is then further reacted with other sets of *p*-substituted styrenes via Heck coupling to produce a set of R'VinylStilbeneOS compounds. The R' = NH₂ compound is then reacted with 3,5-dibromo or dinitrobenzoyl chloride to produce hexadecafunctional 3-D stars. These synthetic methods provide perfect single core and then core-shell 3-D stars including in the third generation branch points such that these molecules can be used for the synthesis of new dendrimers or hyperbranched molecules. Further, the first sets of materials are fully conjugated. Investigation of the UV-vis absorption, photoluminescence, and two-photon absorption properties of the R'VinylStilbeneOS compounds, especially where R' = NH₂, reveals exceptional red-shifts (120 nm), charge-transfer behavior, and excellent two-photon absorption properties that may suggest that the silica core serves the role of electron acceptor in the system and interacts equally with all eight organic moieties. This observation may imply 3-D conjugation through the core.

Introduction

There is widespread interest in developing building blocks for constructing materials with architectures tailored at nanometer length scales.^{1–5} The motivation is multifold in that the ability to assemble materials at such length scales should provide high reproducibility of global properties and the opportunity to precisely predict and fine-tune those properties.^{6–10} Still another motivation is the potential to identify new properties in nanoscale building blocks not available in the bulk but that can then be used to create entirely new materials by ordering these nanocomponents over large length scales or simply using them as is.^{10,11}

In principle, nanometer-sized molecules with high symmetry, functionality, and a means to modify that functionality

at will to aid in assembling 1-, 2-, or 3-D structures nanometer by nanometer would seem to offer the best potential for complete control of properties over all length scales. To this end, molecules with cubic symmetry could be exceptional candidates to develop routes to well-defined, molecular nanobuilding blocks.

To date, only the cubane family of compounds and cubic silsesquioxanes, Q₈ (ROSiO_{1.5})₈ and T₈ (RSiO_{1.5})₈, offer the requisite symmetry.^{8,9,12–42} Of these, only the silsesquioxanes are easily prepared in large quantities and readily octafunctionalized. For example, the Q₈ compound [HMe₂SiOSiO_{1.5}]₈ (OHS) has been functionalized by hydrosilylation to introduce alkyl, vinyl, epoxy, alcohol, isocyanate, and acrylate groups.^{25–35} Sets of silsesquioxanes based on OHS have recently been used to synthesize novel luminescent molecules.^{43–45} OHS has also been transformed into bifunctional “Janus” compounds including one that melts and then self-condenses.⁴²

Polyfunctional T₈ and even T₁₂ systems have also been made including R = R'Phenyl derivatives where R' = amine,

[†] Macromolecular Science and Engineering Center.

[‡] Department of Chemistry.

[§] Department of Materials Science and Engineering.

- (1) Seidel, S. R.; Stang, P. J. *Acc. Chem. Res.* **2002**, *35*, 972.
- (2) Addicott, C.; Das, N.; Stang, P. J. *Inorg. Chem.* **2004**, *43*, 5335.
- (3) Stewart, M. D.; Willson, C. G. *MRS Bull.* **2005**, *30*, 947.
- (4) Levins, C. G.; Schafmeister, C. F. *J. Am. Chem. Soc.* **2003**, *125*, 4702.
- (5) Yaghi, O. M.; Li, H.; Davis, C.; Richardson, D.; Groy, T. L. *Acc. Chem. Res.* **1998**, *31*, 474.
- (6) Lanznaster, M.; Heeg, M. J.; Yee, G. T.; McGarvey, B. R.; Verani, C. N. *Inorg. Chem.* **2007**, *46*, 72.
- (7) Laine, R. M.; Choi, J.; Lee, I. *Adv. Mater.* **2001**, *13*, 800.
- (8) Eaton, P. E. *Angew. Chem., Int. Ed. Engl.* **1992**, *31*, 1421.
- (9) Roll, M. F.; Asuncion, M. Z.; Kampf, J.; Laine, R. M. *ACS Nano* **2008**, *2*, 320.

- (10) Morin, J.-F.; Shirai, Y.; Tour, J. M. *Org. Lett.* **2006**, *8*, 1713.
- (11) Sasaki, T.; Osgood, A. J.; Alemany, L. B.; Kelly, K. F.; Tour, J. M. *Org. Lett.* **2008**, *10*, 229.
- (12) Detken, A.; Zimmerman, H.; Haeberlen, U.; Poupko, R.; Luz, Z. *J. Phys. Chem.* **1996**, *100*, 9598.
- (13) Yildirim, T.; Gehring, P. M.; Neumann, D. A.; Eaton, P. E.; Emrick, T. *Carbon* **1998**, *36*, 809.

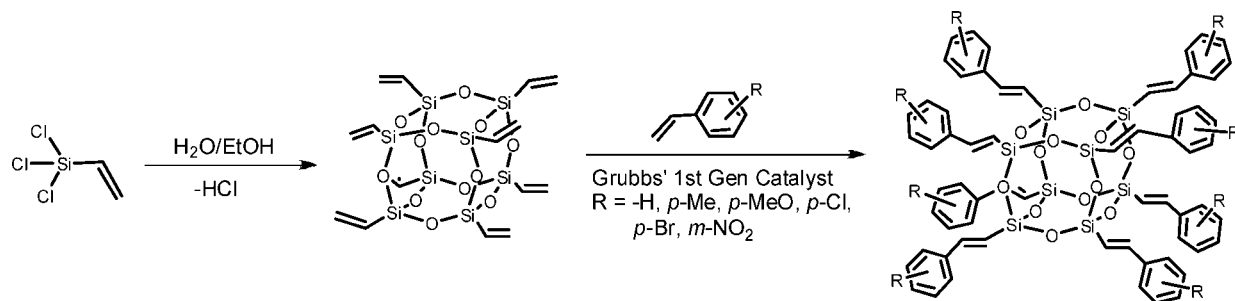


Figure 1. Synthesis of OVS (30–40% yield) and RStyrenyIOS.

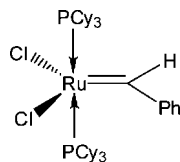


Figure 2. Grubbs type 1 catalyst.

halogen, methacrylate, vinyl, alkynyl, arenyl, and so forth.^{31,32,36,38–40} Combinations of Q₈ and T₈ epoxy/amine systems provide materials with physical properties that can be tailored by modifying functionalization at nanometer length scales.^{7,29,30,40}

A further advantage is the single crystal silica core, which provides the heat capacity of silica making these systems unusually robust.³⁶ The 3-D symmetry also provides materials that are very soluble and therefore easily purified by standard methods.

In this paper, motivated by work by Marciniec et al.,⁴⁶ Feher et al.,⁴⁷ and Sellinger et al.⁴⁸ on octavinylsilsesquioxane (OVS, [vinylSiO_{1.5}]₈), our efforts target the development of nanobuilding blocks for nanoconstruction but also access to perfect and perfectly symmetrical 3-D stars built on OVS cores. We report here, as illustrated in Figures 1–4 functionalization of OVS with functionalized styrenes via cross-metathesis reactions, forming the first generation star materials, octa(RStyrenyl)silsesquioxane (RStyrenyIOS). A variety of R groups are used to demonstrate the versatility of this reaction.

Octa(*p*-bromostyrenyl)silsesquioxane (BrStyrenyIOS) is further functionalized via Heck reactions with functionalized

styrenes to give perfectly symmetrical and perfect octa-(R'vinylstilbene)silsesquioxane (R'VinylStilbeneOS), second generation stars. A further goal of the work initiated here is to methodically explore the luminescence properties of these materials based on the initial findings of Sellinger et al.,⁴⁸ who are the only researchers to examine the luminescence properties of silsesquioxanes where the cage is conjugated to the organic lumiphore. Finally, octa(*p*-aminovinylstilbene)silsesquioxane (NH₂VinylStilbeneOS) is reacted with difunctional benzoylchlorides to give octa(R''₂-benzamidevinylstilbene)silsesquioxane (R''₂-BenzamideOS), third generation molecules with increased functional group density and potential for further functionalization and branching.

Experimental Section

Materials. Methylene chloride (CH₂Cl₂) was purchased from Fisher and distilled from CaH₂ under N₂ prior to use. OVS was synthesized according to procedures developed by Harrison and Hall.⁵⁰ *p*-Vinylstilbene was synthesized according to the literature.⁵¹ A first generation Grubbs catalyst [RuCl₂(=CHPh)(PCy₃)₂] was purchased from Aldrich. All other chemicals were purchased from Aldrich or Fisher and used as received.

General Metathesis Reactions of OVS. To a dry 10 mL Schlenk flask under N₂ was added 0.40 g (5.1 mmol –CH=CH₂) of OVS and 21.0 mg (0.0265 mmol, 0.5 mol %) of first generation Grubbs catalyst. Dry CH₂Cl₂ (6 mL) was added by syringe followed by R-styrene (7.56 mmol). The mixture was stirred at room temperature for 72 h and then quenched by precipitation into 200 mL of methanol. The solution was then filtered, and the product was further purified by column chromatography (silica, CH₂Cl₂).

General Heck Reaction of BrStyrenyIOS. To a dry 50 mL Schlenk flask under N₂ was added 0.50 g (2.14 mmol-Br) of BrStyrenyIOS, 19 mg (0.04 mmol) of Pd[P(*t*-Bu)₃]₂, and 18 mg (0.02 mmol) of Pd₂(dba)₃. 1,4-Dioxane (10 mL) was then added by syringe, followed by NCy₂Me (2.11 mmol, 0.45 mL) and R-styrene (6.41 mmol). The mixture was stirred at room temperature for 72 h and then quenched by filtering through 1 cm Celite, which was washed with 5 mL of THF. The solution was then precipitated into 200 mL of methanol and filtered and the solid redissolved in 10 mL of THF. This solution was then filtered again through a 1 cm Celite column to remove any remaining Pd particles and reprecipitated into 200 mL of methanol. The product was further purified by column chromatography (silica, 1:10 THF:hexane).

Reaction of NH₂VinylStilbeneOS with Difunctional Benzoylchlorides. To a dry 10 mL Schlenk flask under N₂ was added 0.1 g (0.37 mmol-NH₂) of NH₂VinylStilbeneOS dissolved in 1 mL of THF. A solution of 0.74 mmol of the corresponding benzoylchloride in 1 mL of THF was then added to the flask via syringe, followed by 0.05 mL (0.36 mmol) of triethylamine. The mixture was stirred

- (14) For recent reviews see (a) Voronkov, M. G.; Lavrent'yev, V. I. *Top. Curr. Chem.* **1982**, 102, 199. (b) Baney, R. H.; Itoh, M.; Sakakibara, A.; Suzuki, T. *Chem. Rev.* **1995**, 95, 1409. (c) Provatas, A.; Matison, J. G. *Trends Polym. Sci.* **1997**, 5, 327. (d) Loy, D. A.; Shea, K. J. *Chem. Rev.* **1995**, 95, 1431. (e) Lichtenhan, J. In *Polymeric Materials Encyclopedia*; Salmone, J. C., Ed.; CRC Press: New York, 1996; Vol. 10, p 7768. (f) Laine, R. M. *J. Mater. Chem.* **2005**, 3725. (g) Calzaferri, G. In *Tailor-made Silicon-oxygen Compounds, From Molecules to Materials*; Corriu, R.; Jutzi, P., Eds.; Publ. Friedr. Vieweg & Sohn, mbH, Braunschweig/Weisbaden, Germany, 1996; p 149.
- (15) (a) Lichtenhan, J. D.; Vu, H. Q.; Carter, J. A.; Gilman, J. W.; Feher, F. J. *Macromolecules* **1993**, 26, 2141. (b) Gilman, J. W.; Schlitzer, D. S.; Lichtenhan, J. D. *J. Appl. Polym. Sci.* **1996**, 60, 591. (c) Gonzalez, R. I.; Phillips, S. H.; Hoflund, G. B. *J. Spacecraft Rockets* **2000**, 37, 463.
- (16) (a) Weidner, R.; Zeller, N.; Deubzer, B.; Frey, V. U.S. Patent 5,047,492, Sept. 1991. (b) Dathe, S.; Popowski, E.; Sonnek, G.; Feiher, T.; Jancke, H.; Schelm, U. Eur. Patent 0,348,705 A 1, 1989. (c) Freyer, C.; Wolferseder, J.; Peetz, U. Eur. Patent, 0,624,691 A 1, 1993.
- (17) (a) Zhang, Y.; Lee, S. H.; Liang, K.; Toghiani, H.; Pittman, C. U. *Polymer* **2006**, 47, 2984. (b) Patel, R. R.; Mohanraj, R.; Pittman, C. U. *J. Polym. Sci., Part B: Polym. Phys.* **2006**, 44, 234. (c) Liang, K.; Li, G. Z.; Toghiani, H.; Koo, J. H.; Pittman, C. U. *Chem. Mater.* **2006**, 18, 301.

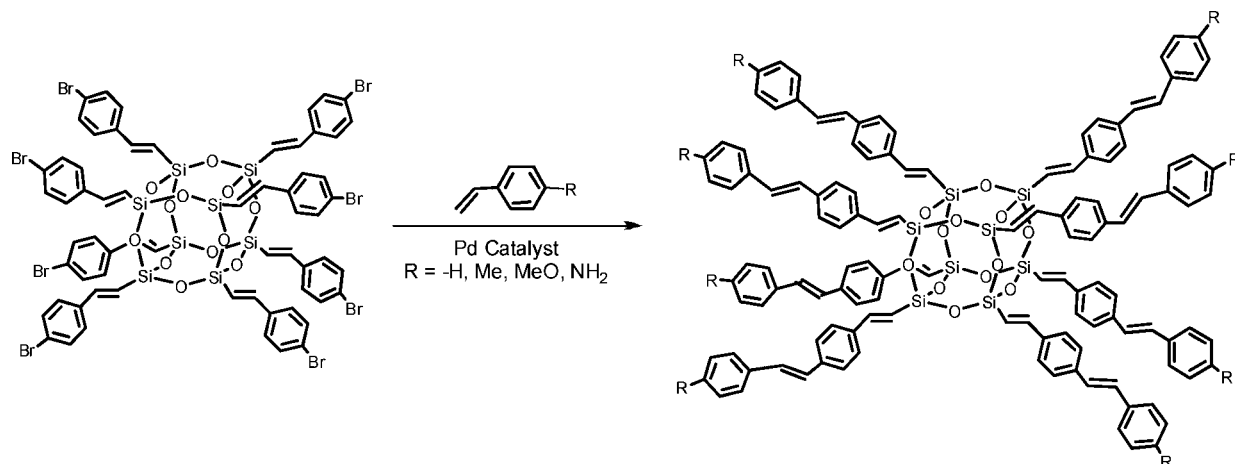


Figure 3. Synthesis of R'VinylStilbeneOS from BrStyrenylOS.

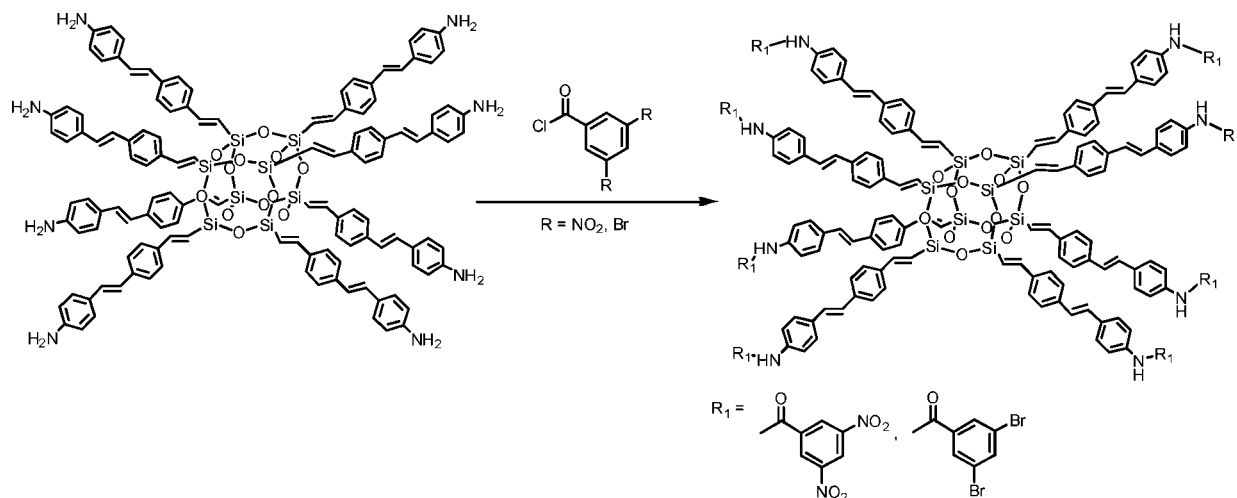


Figure 4. Synthesis of R''₂-BenzamideOS from NH₂VinylStilbeneOS.

at room temperature for 24 h and then quenched by filtering through 1 cm Celite. The filtrate was then precipitated into 50 mL of hexane.

Analytical data for all of the synthesized compounds are given in the Results and Discussion section below.

Analytical Methods. *Gel Permeation Chromatography (GPC).* GPC analyses were done on a Waters 440 system equipped with Waters Styragel columns (7.8 × 300, HT 0.5, 2, 3, 4) with RI detection using Waters refractometer and THF as solvent. The system was calibrated using polystyrene standards and toluene as reference.

Nuclear Magnetic Resonance. All ¹H and ¹³C NMR were performed in CDCl₃ or DMSO-*d*₆ and recorded on a Varian INOVA 400 MHz spectrometer. All ²⁹Si NMRs were performed in CDCl₃

or DMSO-*d*₆ and recorded on a Bruker Avance DRX-500 spectrometer. ¹H NMR spectra were collected at 400 MHz using a 6000 Hz spectral width, a relaxation delay of 3.5 s, 30k data points, a pulse width of 38°, and TMS (0.00 ppm) as the internal reference. ¹³C NMR spectra were collected at 100 MHz using a 25 000 Hz spectral width, a relaxation delay of 1.5 s, 75k data points, a pulse width of 40°, and TMS (0.00 ppm) as the internal reference. ²⁹Si NMR spectra were collected at 100 MHz using a 14 000 Hz spectral width, a relaxation delay of 20 s, 65k data points, a pulse width of 7°, and TMS (0.00 ppm) as the internal reference.

- (18) Stewart, M. D.; Wetzel, J. T.; Schmid, G. M.; Parmieri, F.; Thompson, E.; Kim, E. K.; Wang, D.; Sotodoe, K.; Jen, K.; Johnson, S. C.; Hao, J.; Dickey, M. D.; Nishimura, Y.; Laine, R. M.; Resnick, D. J.; Willson, C. G. *Proc. SPIE-Int. Soc. Opt. Eng.* **2005**, 219, 5751.
- (19) (a) Hasegawa, I.; Sakka, S.; Sugahara, Y.; Kuroda, K.; Kato, C. *J. Chem. Soc., Chem. Commun.* **1989**, 208. (b) Hasegawa, I.; Motojima, S. *J. Organomet. Chem.* **1992**, 441, 373. (c) Hasegawa, I.; Sakka, S. *Chem. Lett.* **1988**, 1319.
- (20) Agaskar, P. A. *Inorg. Chem.* **1991**, 30, 2707.
- (21) (a) Hoebbel, D.; Endres, K.; Reinert, T.; Pitsch, I. *J. Noncryst. Solids* **1994**, 176, 179. (b) Hoebbel, D.; Pitsch, I.; Heidmann, D. *Eurolog '91, Elsevier Sci. Publ.* **1992**, 467.
- (22) (a) Hong, B.; Thoms, T. P. S.; Murfee, H. J.; Lebrun, M. J. *Inorg. Chem.* **1997**, 36, 6146. (b) Feher, F. J.; Wyndham, K. D. *Chem. Commun.* **1998**, 323. (c) Dvornic, P. R.; Hartmann-Thompson, C.; Keinath, S. E.; Hill, E. J. *Macromolecules* **2004**, 37, 7818.

- (23) (a) Waddon, A. J.; Coughlin, E. B. *Chem. Mater.* **2003**, 15, 4555. (b) Cardoen, G.; Coughlin, E. B. *Macromolecules* **2004**, 37, 5123.
- (24) (a) Fu, B. X.; Hsiao, B. S.; White, H.; Rafailovich, M.; Mather, P.; Joen, H. G.; Phillips, S.; Lichtenhan, J.; Schwab, J. *Polym. Int.* **2000**, 49, 437. (b) Fu, B. X.; Zhang, W.; Hsiao, B. S.; Rafailovich, M.; Sokolov, J.; Johansson, G.; Sauer, B. B.; Phillips, S.; Blanski, R. *High Perform. Polym.* **2001**, 12, 565.
- (25) (a) Imae, I.; Kawakami, Y. *J. Mater. Chem.* **2005**, 15, 4581. (b) Lin, H.-C.; Kuo, S.-W.; Huang, C.-F.; Chang, F.-C. *Macromol. Rapid Commun.* **2006**, 27, 537.
- (26) (a) Baker, E. S.; Gidden, J.; Anderson, S. E.; Haddad, T. S.; Bowers, M. T. *Nano Lett.* **2004**, 4, 779. (b) Fu, B. X.; Lee, A.; Haddad, T. S. *Macromolecules* **2004**, 37, 5211. (c) Kopesky, E. T.; Haddad, T. S.; Cohen, R. E.; McKinley, G. H. *Macromolecules* **2004**, 37, 8992. (d) Tuteja, A.; Choi, W.; Ma, M.; Mabry, J. M.; Mazella, S. A.; Rutledge, G. C.; McKinley, G. H.; Cohen, R. E. *Science* **2007**, 318, 1618.
- (27) (a) Kim, G.-M.; Qin, H.; Fang, X.; Sun, F. C.; Mather, P. T. *J. Poly. Sci., Part B: Polym. Phys.* **2003**, 41, 3299. (b) Kim, B. S.; Mather, P. T. *Macromolecules* **2002**, 35, 8378.

Thermogravimetric Analysis (TGA). TGA was run on a 2960 simultaneous DTA-TGA instrument (TA Instruments, Inc., New Castle, DE). Samples (15–25 mg) were loaded in alumina pans and ramped at 10 °C/min to 1000 °C under dry air with a flow rate of 60 mL/min.

Differential Scanning Calorimetry (DSC). DSC was performed on materials using a DSC 2910 (TA Instruments, Inc., New Castle, DE). The N₂ flow rate was 60 mL/min. The sample (5–10 mg) was placed in a pan without capping and ramped to the desired temperature at a rate of 10 °C/min. The heat flow difference between a blank pan and the sample pan was recorded.

Matrix-Assisted Laser Desorption/Time-of-Flight Spectrometry (MALDI-ToF). MALDI-ToF was done on a Micromass ToFSpec-2E equipped with a 337 nm nitrogen laser in positive-ion reflectron mode using poly(ethylene glycol) as calibration standard, dithranol as matrix, and AgNO₃ as ion source. Samples were prepared by mixing solutions of 5 parts matrix (10 mg/mL in THF), 5 parts sample (1 mg/mL in THF), and 1 part AgNO₃ (2.5 mg/mL in water) and blotting the mixture on the target plate.

UV-vis Spectrometry. UV-vis spectra were taken on a Shimadzu UV-1601 UV-vis transmission spectrometer in CH₂Cl₂. Samples were dissolved in CH₂Cl₂ and diluted to a concentration (10^{−3}–10^{−4} M) where the absorption maximum was less than 10% for a 1 cm path length.

Photoluminescence Spectrometry. Photoluminescent spectra were taken on a Fluoromax-2 fluorimeter in CH₂Cl₂ using 260 nm excitation for R-styrenylos and 320 nm excitation for R-vinylstilbeneOS. Samples of RStyrenylos from UV-vis spectroscopy were

used without dilution, while samples of R'VinylstilbeneOS from UV-vis spectroscopy were diluted (10^{−5} to 10^{−6} M) to avoid excimer formation and fluorimeter detector saturation.

Photoluminescence Quantum Yields (Φ_{PL}). Φ_{PL} was determined by a modification of the relative method described by Demas and Crosby⁵² using anthracene⁵³ and 9,10-diphenylanthracene⁵⁴ as references. The absorption at 320 nm was determined for each material at three different concentrations (maximum absorption of 20%). These samples were then diluted by equal amounts to avoid fluorimeter saturation and excimer formation, and the total area of the emission spectrum was calculated. For each solution, absorption and emission measurements were repeated a minimum of two times and averaged. The slope of a plot of emission versus absorption was determined for each material and relative quantum efficiency calculated according to the equation

$$\Phi_{\text{PL}}(x) = \left(\frac{A_s}{A_x} \right) \left(\frac{F_x}{F_s} \right) \left(\frac{n_x}{n_s} \right)^2 \Phi_{\text{PL}}(s)$$

where Φ_{PL} is the quantum yield, *A* is the absorption at the excitation wavelength, *F* is the total integrated emission, and *n* is the refractive index of the solution, which can be approximated to be the refractive index of the solvent, considering the low concentration of the solution. Subscripts *x* and *s* refer to the sample to be measured and the reference, respectively.

Two-Photon Studies. *a. Steady State Measurements.* All compounds were dissolved in tetrahydrofuran (THF) (Sigma-Aldrich, spectrophotometric grade) for carrying out the optical measurements. The absorption spectra of the molecules were measured using an Agilent (Model No. 8341) spectrophotometer. The fluorescence spectra were acquired using a Spex-fluorolog spectrofluorimeter. The quantum yields of the molecules were measured using a known procedure. Bis-MSB [*p*-bis(*o*-methyl-styryl) benzene] has been used as the standard. The absorbance was limited to equal to or less than 0.1. These measurements may have some error due to sensitivity of the fluorescence spectrophotometer and other environmental conditions.

b. Two-Photon Excited Fluorescence Measurements. To measure the two photon absorption cross sections, we followed the two photon excited fluorescence (TPEF) method.⁵⁵ Bis-MSB dissolved in cyclohexane (620–710 nm) and C-307 in methanol (710–800 nm) were used as references for measuring TPA cross sections at different wavelength regions. The laser used for the measurements was an amplified femtosecond laser (Spitfire, Spectraphysics) pumped optical parametric amplifier (OPA-800C, Spectraphysics) which gives tunable wavelengths from 300 to 2000 nm. The input power from the laser was varied by using a neutral density filter. An iris was placed prior to the neutral density filter to ensure a circular beam. The beam was directed onto the sample cell (quartz cuvette, 0.5 cm path length), and the resultant fluorescence was collected in a direction perpendicular to the incident beam. A 1 in. focal length plano-convex lens was used to direct the collected fluorescence into a monochromator. The output from the monochromator was coupled to a PMT. The photons were converted into counts by a photon counting unit. A logarithmic plot between collected fluorescence photons and input intensity gave a slope of two, ensuring a quadratic dependence between the same. The intercept enabled us to calculate the two photon absorption cross sections at different wavelengths.

- (28) Selinger, A.; Laine, R. M. *Macromolecules* **1996**, *29*, 2327.
- (29) Choi, J.; Harcup, J.; Yee, A. F.; Zhu, Q.; Laine, R. M. *J. Am. Chem. Soc.* **2001**, *123*, 11420.
- (30) Choi, J.; Yee, A. F.; Laine, R. M. *Macromolecules* **2003**, *15*, 5666.
- (31) Tamaki, R.; Tanaka, Y.; Asuncion, M. Z.; Choi, J.; Laine, R. M. *J. Am. Chem. Soc.* **2001**, *123*, 12416.
- (32) (a) Tamaki, R.; Choi, J.; Laine, R. M. *Chem. Mater.* **2003**, *15*, 793. (b) Choi, J.; Tamaki, R.; Kim, S. G.; Laine, R. M. *Chem. Mater.* **2003**, *15*, 3365.
- (33) Neumann, D.; Fisher, M.; Tran, L.; Matisons, J. G. *J. Am. Chem. Soc.* **2002**, *124*, 13998.
- (34) Maitra, P.; Wunder, S. L. *Chem. Mater.* **2002**, *14*, 4494.
- (35) Mehl, G. H.; Goodby, J. W. *Angew. Chem.* **1996**, *35*, 2641.
- (36) Brick, C. M.; Ouchi, Y.; Chujo, Y.; Laine, R. M. *Macromolecules* **2005**, *38*, 4661.
- (37) Zhang, Z. L.; Horsch, M. A.; Lamm, M. H.; Glotzer, S. C. *Nano Lett.* **2003**, *3*, 1341.
- (38) Takahashi, K.; Sulaiman, S.; Katzenstein, J. M.; Snoblen, S.; Laine, R. M. *Aust. J. Chem.* **2006**, *59*, 564.
- (39) Sulaiman, S.; Brick, C. M.; De Sana, C. M.; Katzenstein, J. M.; Laine, R. M.; Basheer, R. A. *Macromolecules* **2006**, *39*, 5167.
- (40) Asuncion, M. Z.; Laine, R. M. *Macromolecules* **2007**, *40*, 555.
- (41) Brick, C. M.; Chan, E. R.; Glotzer, S. C.; Martin, D. C.; Laine, R. M. *Adv. Mater.* **2007**, *19*, 82.
- (42) (a) Takamura, N.; Viculis, L.; Laine, R. M. *Polym. Int.* **2007**, *56*, 1378. (b) Laine, R. M.; Roll, M.; Asuncion, M.; Sulaiman, S.; Popova, V.; Bartz, D.; Krug, D. J.; Mutin, P. H. *J. Sol-Gel Sci. Technol.* **2008**, *46*, 335.
- (43) Imae, I.; Kawakami, Y. *J. Mater. Chem.* **2005**, *15*, 4581.
- (44) Cho, H.-J.; Hwang, D.-H.; Lee, J.-I.; Jung, Y.-K.; Park, J.-H.; Lee, J.; Lee, S.-K.; Shim, H.-K. *Chem. Mater.* **2006**, *18*, 3780.
- (45) Froehlich, J. D.; Young, R.; Nakamura, T.; Ohmori, Y.; Li, S.; Mochizuki, A.; Lauters, M. *Chem. Mater.* **2007**, *19*, 4991.
- (46) (a) Marciniak, B.; Pietraszuk, C. *Curr. Org. Chem.* **2003**, *7*, 691. (b) Kujawa-Welten, M.; Pietraszuk, C.; Marciniak, B. *Organometallics* **2002**, *21*, 840. (c) Itami, Y.; Marciniak, B.; Kubicki, M. *Chem. Eur. J.* **2004**, *10*, 1239.
- (47) Feher, F. J.; Soulivong, D.; Eklund, A. G.; Wyndham, K. D. *Chem. Commun.* **1997**, 1185.
- (48) (a) Sellinger, A.; Tamaki, R.; Laine, R. M.; Ueno, K.; Tanabe, H.; Williams, E.; Jabbour, G. E. *Chem. Commun.* **2005**, 3700. (b) Lo, M. Y.; Zhen, C.; Lauters, M.; Jabbour, G. E.; Sellinger, A. *J. Am. Chem. Soc.* **2007**, *129*, 5808.
- (49) Grubbs, R. H. *Handbook of Metathesis*; Wiley-VCH: New York, 2003.
- (50) Harrison, P. G.; Hall, C. *Main Group Met. Chem.* **1997**, *20*, 515.
- (51) Bezou, P.; Hilberer, A.; Hadziioannou, G. *Synthesis* **1996**, *4*, 449.

(52) Crosby, G. A.; Demas, J. N. *J. Phys. Chem.* **1971**, *75*, 991.

(53) *Standards for Fluorescence Spectrometry*; Miller, J. N., Ed.; Chapman and Hall: London, 1981.

(54) Hamai, S.; Hirayama, F. *J. Phys. Chem.* **1983**, *87*, 83.

(55) Xu, C.; Webb, W. W. *J. Opt. Soc. Am. B* **1996**, *13*, 481.

Table 1. Characterization Data for RStyrenyIOS

R group	m/z (Ag^+ adduct)		GPC				ceramic yield (%)		$T_{d5\%}$ ($^{\circ}\text{C}$)	T_m ($^{\circ}\text{C}$, N_2)
	MALDI	calcd	M_n	M_w	FW	PDI	actual	calcd		
H	1349.2	1349.7	1025	1034	1241.8	1.01	38.6	38.7	395	270
<i>p</i> -Me (octamer)	1461.6	1461.9	1257	1278	1354.0	1.02	33.5	35.5	283	315
<i>p</i> -MeO	1589.1	1589.9	1262	1283	1482.0	1.02	33.6	32.4	323	345
<i>p</i> -Cl	1626.8	1625.2	1387	1403	1517.4	1.01	31.5	31.7	362	310
<i>p</i> -Br	1981.3	1980.8	1321	1350	1872.0	1.02	25.7	25.6	318	330
<i>m</i> -NO ₂	1710.1	1709.7	1561	1607	1601.8	1.03	29.8	30.0	331	n.a.

Table 2. Characterization Data for R'VinylStilbeneOS

R' group	m/z (Ag^+ adduct)		GPC				ceramic yield (%)		$T_{d5\%}$ ($^{\circ}\text{C}$)
	MALDI	calcd	M_n	M_w	FW	PDI	calcd	actual	
H	2162.7	2166.7	1511	1597	2058.9	1.06	23.4	23.8	400
<i>p</i> -Me	2279.9	2279.0	1775	1876	2171.1	1.06	22.1	21.1	390
<i>p</i> -MeO	2404.6	2406.9	1880	2096	2299.1	1.12	20.9	22.6	315
<i>p</i> -NH ₂	2287.6	2286.9	1374	1549	2179.0	1.13	22.1	20.1	345

Results and Discussion

The objectives of the work undertaken here were (1) to explore the utility of combining metathesis and Heck chemistry to produce perfect, conjugated core-shell stars from OVS; (2) to realize functionality in the first and second shells for further elaboration; (3) to develop general synthetic routes to branch points providing access to octa- and hexadeca-functional 3-D cores as starting points for the synthesis of more complex stars, dendrimers, or hyper-branched molecules and nanostructured materials therefrom; and (4) to investigate the photoluminescence properties of these novel system for comparison with more highly conjugated appended aromatics as described by Sellinger et al.⁴⁸

In the following sections we discuss the synthesis and characterization of these materials and their photoluminescence properties in order of their complexity starting with the styrenyl₈T₈ systems, going to the vinylstilbenes, and ending with hexadecafunctionalized stars.

Synthesis Methods. Cross-metathesis reactions were carried out using commercially available functionalized styrenes and a first generation Grubbs catalyst.⁴⁹ The reaction mixture was stirred for 72 h to ensure complete conversion of the vinyl groups. Since metathesis is an equilibrium reaction, the reaction can be driven to >99% conversion of OVS to RStyrenyIOS by blowing a gentle stream of N₂ above the reaction mixture to remove ethylene formed.

Heck coupling was run using R-styrenes having functional groups with different electron-donor groups using a 2:1 molar mixture of Pd[P(*t*-Bu)₃]₂ and Pd₂(dba)₃ as the catalyst system.⁵⁶

The amino derivative, NH₂VinylStilbenOS, was acylated with 3,5-difunctional (NO₂- or Br-) benzoyl chloride using a standard procedure to provide the first examples of a branch point at the ends of the star arms. The nitro derivative can be reduced to the amino derivative, which then introduces 16 functional groups as a first generation 3-D dendrimer as will be reported later. The bromo derivatives should permit further functionalization via various coupling reactions. These compounds also may serve as 3-D cores for forming dendrimers.

Solubilities. The RStyrenyIOS and R'VinylStilbeneOS compounds are soluble in various organic solvents such as THF, toluene, dioxane, CH₂Cl₂, and CHCl₃. The R''₂-BenzamideOS compounds (third generation) are soluble in polar solvents such as THF and DMSO.

Characterization of (RStyrenyl)OS, (R'VinylStilbene)-OS, and R''₂BenzamideOS. *MALDI-ToF Data.* MALDI-ToF data for first and second generation stars are given in Tables 1 (RStyrenyIOS) and 2 (R'VinylStilbeneOS). Figure 5 provides representative spectra for RStyrenyIOS. With the exception of the MeStyrenyIOS compound, all the RStyrenyIOS compounds are perfectly octa-substituted. For the second generation compounds, no double Heck reactions on BrStyrenyIOS akin to those targeted by Sellinger et al.⁴⁸ are observed, due to the large excess of R-styrene used. We were not able to obtain MALDI-ToF data for R''₂BenzamideOS, but ¹H- and ¹³C NMR spectra of these compounds confirm their complete conversion from their parent material (NH₂VinylStilbeneOS).

²⁹Si NMR. ²⁹Si NMR data for selected compound can be found in the Supporting Information (Tables S-3, S-6, and S-9). All of the decoupled spectra show a single resonance at ~ -78 ppm, which indicates that (a) all of the silicon atoms in each silsesquioxane core are magnetically equivalent and (b) the magnetic environment around the silicon atoms does not change from the first generation compounds to the second and third generation compounds. This is expected

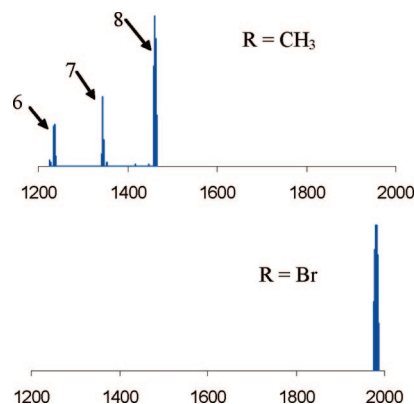


Figure 5. MALDI-ToF spectra for (RStyrenyl)OS. Octa-substitution was observed for all RStyrenyIOS compounds except (a) MeStyrenyIOS; (b) BrStyrenyIOS shown for comparison.

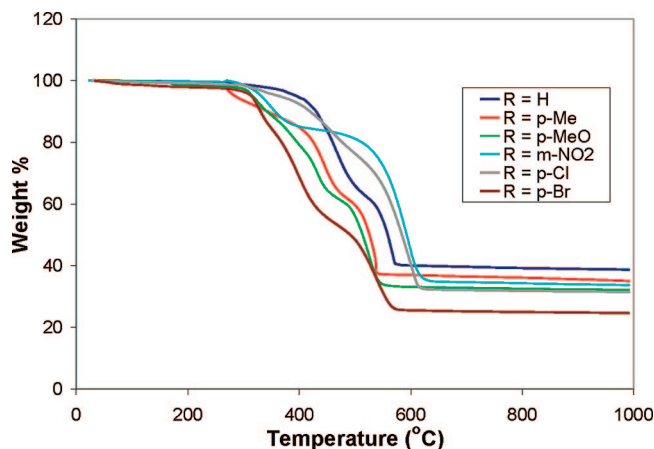
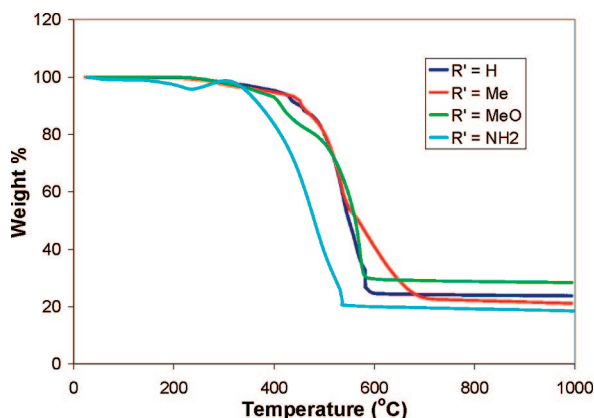
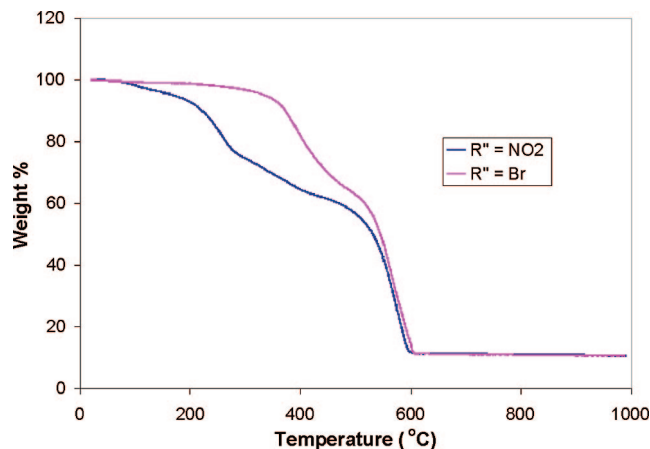
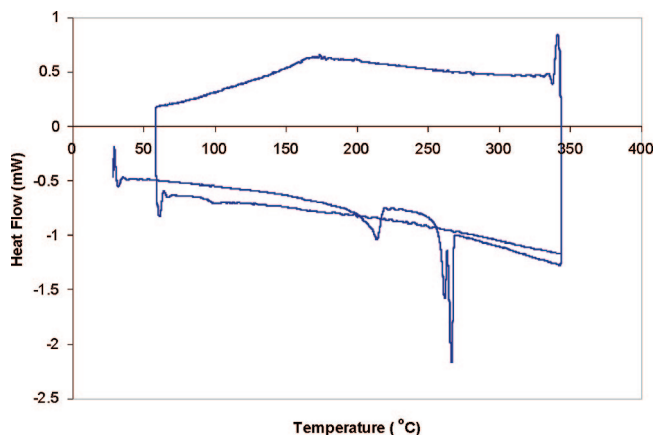
Table 3. Characterization Data for R''₂BenzamideOS

R'' group	GPC				ceramic yield (%)		<i>T</i> _{d5%} (°C)
	<i>M</i> _n	<i>M</i> _w	FW	PDI	calcd	actual	
NO ₂	2003	2089	3087.8	1.04	12.9	10.5	170
Br	2178	2533	3155.6	1.16	11.2	10.5	335

since the different functional groups on the styrenyl moieties of the first generation compounds are too far away from the silicon atoms to influence their magnetic environments. The different functional groups on the second and the third generation compounds are even farther away from the silicon atoms and as such do not have any influence either.

Gel-Permeation Chromatographic (GPCs) Analyses. GPC data are presented in Tables 1–3. These materials exhibit narrow molecular weight distributions, indicating that they retain their silica cube structures. The values of *M*_n and *M*_w as measured by GPC are smaller than the molecular weight measured by MALDI-ToF but expected from GPC characterization of rigid, spherical molecules using flexible, linear standards, based on previous results.³⁶

TGA. TGA was run in air at heating rates of 10 °C/min. Figures 6–8 show the TGA traces for RStyrenylOS, R'VinylStilbeneOS, and R''₂BenzamideOS, respectively. All of the RStyrenylOS compounds are stable in air to >300 °C, with the exception of MeStyrenylOS, due to the presence of the *p*-methyl group which should readily oxidize given its benzylic structure. HStyrenylOS has the highest thermal stability, as expected from its completely aromatic structure.

**Figure 6.** TGA data in air (10 °C/min) for RStyrenylOS.**Figure 7.** TGA data in air (10 °C/min) for R'VinylStilbeneOS.**Figure 8.** TGA data in air (10 °C/min) for R''₂BenzamideOS.**Figure 9.** DSC thermogram of HStyrenylOS.

(NO₂)₂BenzamideOS exhibits a lower onset of mass loss, 330 °C, likely because of loss of the nitro groups. Table 3 summarizes the decomposition temperatures and ceramic yields for R''₂BenzamideOS. As can be seen from the calculated and actual ceramic yields, the compositions of the compounds are in keeping with the MALDI-ToF and GPC data.

The same trend in thermal decomposition is also observed with the second generation materials. With the exception of the amino derivative, the rest of the R'VinylStilbeneOS compounds are air stable to >300 °C. The amino derivative exhibits a mass gain at ~250 °C, which might arise from oxidation of the amino groups.

Thermal Behavior of StyrenylOS. It occurred to us that having a silica core with pendant styrene groups might permit the polymerization of these groups to form a very novel, highly cross-linked polystyrene with perfectly dispersed, monosized nanosilica particles within the polystyrene matrix in considerable contrast to every other type of filled polystyrene.^{57,58}

The first step in these studies was to run DSCs as illustrated in Figure 9 for StyrenylOS. The first heating cycle traces for HStyrenylOS show endotherms near 210 and 260

(57) Lee, J.; Hong, C. K.; Choe, S.; Shim, S. E. *J. Colloid Interface Sci.* **2007**, *310*, 112.

(58) Bachmann, S.; Wang, H.; Albert, K.; Partch, R. *J. Colloid Interface Sci.* **2007**, *309*, 169.

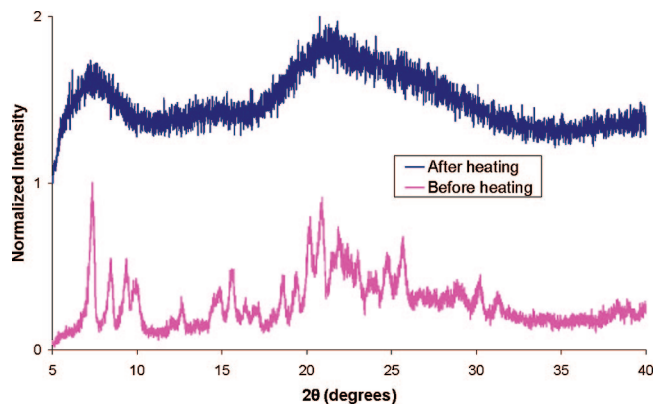


Figure 10. XRD pattern of HStyrenyIOS before and after heating to 300 °C.

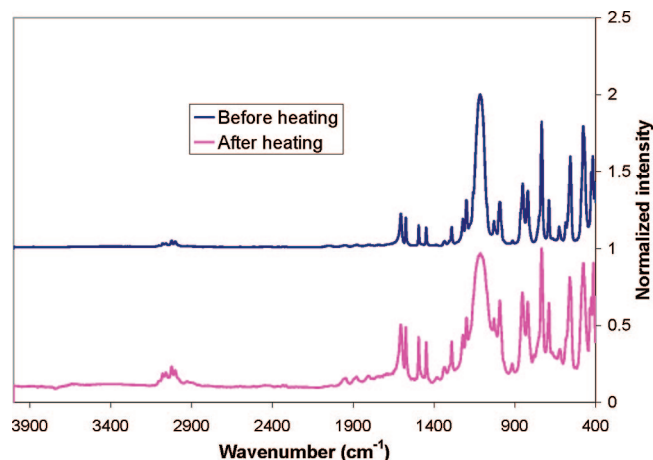


Figure 11. FTIR spectra of HStyrenyIOS before and after heating to 300 °C.

°C but no exotherms on cooling. These endotherms disappear in a second cycle. Hot stage optical microscopy shows that these materials melt over a range of 240–280 °C.

X-ray diffraction (XRD) patterns of HStyrenyIOS before and after heating to 300 °C show that the molten material does not crystallize on cooling leading to the essentially amorphous XRD (Figure 10). This also explains the absence of any exotherms in the cooling cycle and the endotherms in the second heating cycle in the DSC. FTIR spectra (Figure 11) of the material before and after heating to 300 °C do not show any distinct differences. However, after heating the material is no longer soluble, indicating that polymerization occurs at some stage above the melt temperature. The exact polymerization process remains unknown to us; however, it is difficult to envision polymerization of the internal double bonds as being a facile process. As such the second endotherm may be evidence for a very difficult uphill process.

As seen in Figure 12, the $T_{d5\%}$ value for polystyrene is ~290 °C, whereas that for polymerized HStyrenyIOS is 400 °C. This >100 °C increase in oxidative stability could arise for a number of reasons. First, the very uniform dispersion of silica nanoparticles within HStyrenyIOS provides significant added heat capacity, thereby limiting oxidative degradation. Second, as organic is oxidized away from the surface, the remaining residue becomes enriched in silica and provides a barrier to further oxidation. Similar observations

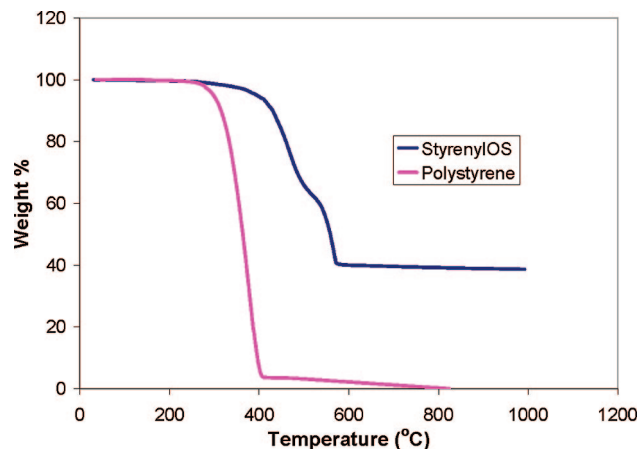


Figure 12. Decomposition of HStyrenyIOS and polystyrene (TGA in air, 10 °C/min).

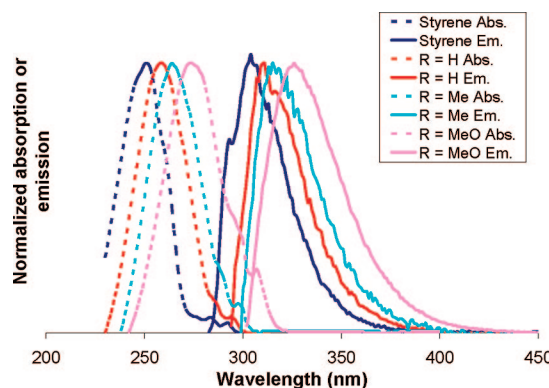


Figure 13. UV absorption and PL emission of RStyrenyIOS in THF.

have been made for silsesquioxane enriched materials exposed to atomic oxygen.¹⁵

Photophysical Properties. UV–vis absorption and photoluminescence (PL) of RStyrenyIOS and R'VinylStilbeneOS in THF are shown above (Figures 13 and 14). Both the absorption and emission spectra show red-shifts from the corresponding small molecule analogues (styrene and *p*-vinylstilbene) untethered to the silsesquioxane core. RStyrenyIOS compounds show smaller red-shifts than R'VinylStilbeneOS compounds (10–40 nm shifts vs 30–80 nm shifts). This is expected because the conjugation lengths for the R'VinylStilbeneOS compounds are twice those of the RStyrenyl-OS compounds. Within both series of compounds, the red-shifts from the small molecules become larger as the functional groups at the silsesquioxane's vertex become more electron-donating. The photoluminescence from NH₂VinylStilbeneOS is quenched on reaction with 3,5-difunctional benzoyl chlorides.

The silsesquioxane core, with a silicon atom attached to three oxygen atoms, has been suggested to act as an electron-withdrawing substituent equivalent to a CF₃ group.⁵⁹ Therefore, one would normally expect to observe a blue-shift for both UV–vis and PL spectra. One possible reason for this shift is considered below.

(59) Feher, F. J.; Budzichowski, T. A. *J. Organomet. Chem.* **1989**, 379, 33.

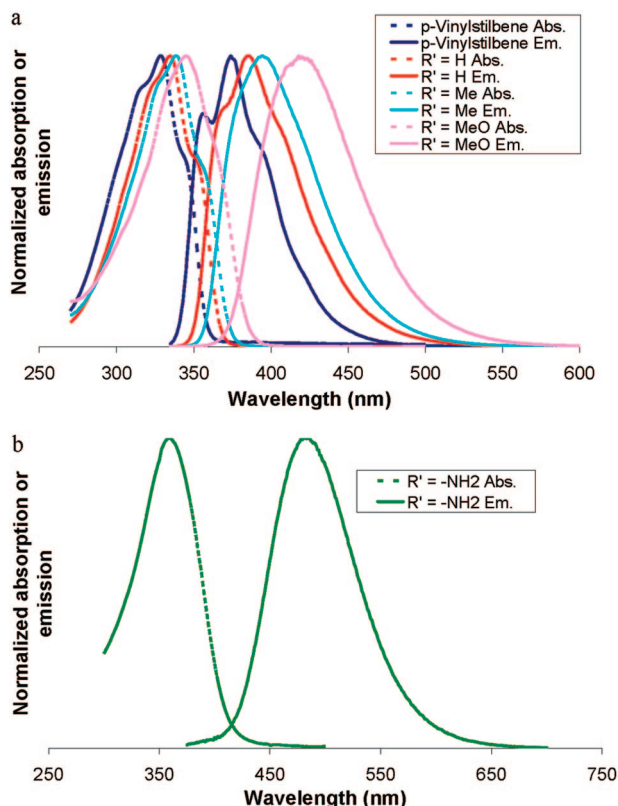


Figure 14. UV-vis and PL spectra of R'VinylStilbeneOS (a: R' = -H, -Me, and -MeO; b: R' = -NH₂) in THF.

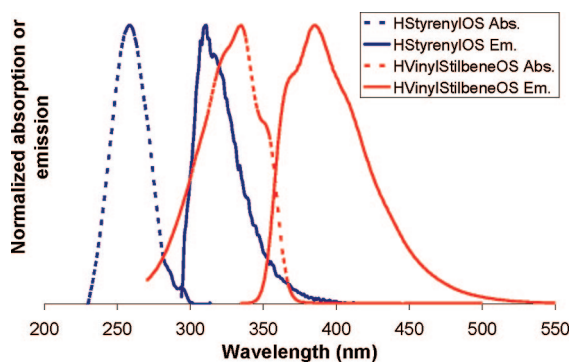


Figure 15. UV-vis and PL spectra of HStyrenylOS and HVinylStilbeneOS.

The absorption and emission spectra of HStyrenylOS and HVinylStilbeneOS in Figure 15 allow us to compare the photophysical properties of the first and second generation materials. The two sets of materials demonstrate similar Stokes shifts of ~50 nm. Both absorption and emission spectra for the second generation materials are red-shifted ~70 nm from those for the first generation materials. The spectra show normal 0–0 transitions typical for conjugated aromatic compounds, suggesting that the silica core has little influence other than the slight red-shifts compared with the organic compounds alone.

The PL quantum yields (Φ_{PL} 's) for RStyrenylOS are very low, as observed from the need to characterize their PL behavior using samples from UV-vis absorption measurements without dilution. Φ_{PL} 's for R'VinylStilbeneOS were measured at 320 nm at high dilution to avoid the formation

of aggregates in solution. Φ_{PL} 's were calculated using anthracene and 9,10-diphenylanthracene as standards.^{52–54} Their values are shown in Table 4. The observed Φ_{PL} for HVinylStilbeneOS is 36%, which is comparable to that measured for the corresponding small molecule, *p*-vinylstilbene. The measured Φ_{PL} for NH₂VinylStilbeneOS is six times lower as a result of charge transfer (CT) effects in the solution, which partially funnel the energy away from luminescence but greatly improve the two-photon cross section (see Table 5 and Figure S1, Supporting Information), which led to the two photon studies as follows.

Two-Photon Cross-Section Studies. Molecular components assembled in a well-defined three-dimensional geometry can potentially lead to novel electronic, optical, and nonlinear optical properties. Among nonlinear optical properties, two-photon absorption (TPA, a third order optical nonlinearity) has received tremendous research attention in recent years because of its applications in different areas of science.⁶⁰ Several molecular architectures such as branched,^{61–64} dendritic,^{65,66} and macrocyclic topologies^{67,68} have shown enhanced TPA cross-sections over their linear counterparts. It has also been shown that when the chromophores are decorated on silver nanoparticles, there is a strong electronic coupling between the chromophores, thereby enhancing the nonlinear optical properties.⁶⁹ However, when the chromophores are adsorbed on a nanoparticle it is difficult to judge the orientation and geometry of chromophore on the nanoparticle. If the chromophores are covalently attached to a known three-dimensional geometry, it is easy to understand the influence of the molecular orientation as well as charge transfer character on the two-photon absorption properties. To this effect, we have investigated the two-photon absorption properties of the donor–acceptor derivatives of selected vinyl stilbenes shown in Figure 3 using methods described in the Experimental Section.

Steady-State Measurements. As noted above the absorption and emission spectra of the investigated systems dissolved in THF are shown in Figure 14. The corresponding optical properties are summarized in Table 4. It can be noted from the figure that the absorption spectrum of the more polar derivative (NH₂VinylStilbeneOS) has shown structureless and red-shifted absorption when compared to the less polar ones (HVinylStilbeneOS and MeOVinylStilbeneOS), suggesting the involvement of a charge transfer transition.

It can also be observed from Figure S-11, Supporting Information, and Table 4 that the Stoke's shift increases with increases in the strength of donor (from HVinylStilbeneOS to NH₂VinylStilbeneOS) suggesting an increased charge transfer character. The reduction of the quantum yield from HVinylStilbeneOS to NH₂VinylStilbeneOS is also in accordance with the increased charge transfer character of the chromophores. It will be interesting to observe how the

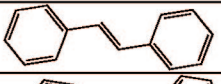
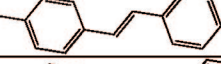
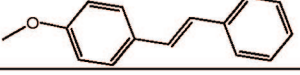
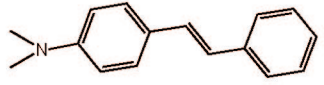
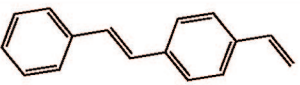
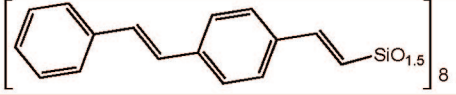
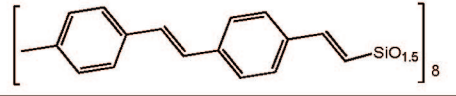
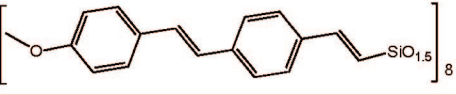
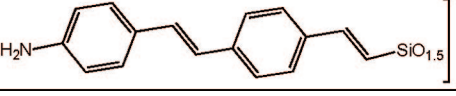
(60) Albota, M.; Beljonne, D.; Bredas, J.-L.; Ehrlich, J. E.; Fu, J.-Y.; Heikal, A. A.; Hess, S. E.; Kogej, T.; Levin, M. D.; Marder, S. R.; McCord-Maughon, D.; Perry, J. W.; Rockel, H.; Rumi, M.; Subramaniam, G.; Webb, W. W.; Wu, X.-L.; Xu, C. *Science* **1998**, *281*, 1653.

(61) (a) Chung, S.-J.; Kim, K.-S.; Lin, T.-C.; He, G. S.; Swiatkiewicz, J.; Prasad, P. N. *J. Phys. Chem. B* **1999**, *103*, 10741. (b) Wang, Y.; He, G. S.; Prasad, P. N.; Goodson, T., III *J. Am. Chem. Soc.* **2005**, *127*, 10128.

Table 4. Spectral Data of RStyrenylOS and R'VinylStilbeneOS

compound	UV λ_{\max} (nm)	PL λ_{\max} (nm)	Φ_{PL} (%)	Stokes shift $\Delta\nu$ (cm^{-1})	δ (GM) @ 780 nm	δ/group (GM)
HStyrenylOS	260	311	n.a.			
MeStyrenylOS	265	315	n.a.			
MeOSStyrenylOS	275	326	n.a.			
Styrene	251	304	n.a.			
HVinylStilbeneOS	335	385	36	3966	25	3.1
MeVinylStilbeneOS	338	394	22			
MeOVinylStilbeneOS	345	418	16	4947	110	13.8
NH ₂ VinylStilbeneOS	358	482	6	6458	810	101
<i>p</i> -Vinylstilbene	329	374	24			

Table 5. Spectral Data of RStyrenylOS and R'VinylStilbeneOS as a Function of Solvent and Two Photon Cross-Sections of Selected Compounds

Compound	Absorption Max (nm)	Emission Max (nm)	Solvent	Φ_{PL} %	Ref
	307	350	CH ₃ CN		70
	311	354	CH ₃ CN		70
	318	375	CH ₃ CN		70
	347	379	Hexane,		71
	349	407	Et ₂ O,		71
	352	418	BuCl,		71
	348	433	EtOH		71
	351	440	CH ₃ CN		71
	324	370	hexane		72
	329	374	CH ₂ Cl ₂	24	72
	325	369	CH ₃ CN		72
	329	375	hexane		72
	335	385	CH ₂ Cl ₂	36	72
	331	388	CH ₃ CN		72
	335	384	hexane		72
	338	394	CH ₂ Cl ₂	22	72
	334	398	CH ₃ CN		72
	339	378	hexane		72
	345	418	CH ₂ Cl ₂	12	72
	343	431	CH ₃ CN		72
	358	482	CH ₂ Cl ₂	6	72
	361	507	CH ₃ CN		72

arrangement of chromophores and the charge transfer character influence the two-photon absorption properties as will be explored at a later date.

Two-Photon Absorption Measurements. TPA cross-sections as a function of wavelength are plotted in Figure S-11, Supporting Information, for all the investigated chromophores. It is clear from the TPA cross-sections that the cross-section increases with the increases in donor strength on the chromophore. It can also be noted that the cross-section per molecule has also increased (Table 4), and it is increased by 35 times when the donor is changed from HVinylStilbeneOS to NH₂VinylStilbeneOS. This 35-fold increase of TPA cross-section can be explained by increased change in dipole-moment term (major factor responsible in sum-over-states formalism).^{62–64}

Solvent Studies. The identification of the CT behavior in NH₂VinylStilbeneOS motivated efforts to explore the effects

- (62) Bhaskar, A.; Ramakrishna, G.; Lu, Z.; Twieg, R. J.; Hales, J. M.; Hagan, D. J.; Van Stryland, E.; Goodson, T., III *J. Am. Chem. Soc.* **2006**, *128*, 11840.
- (63) Ramakrishna, G.; Bhaskar, A.; Goodson, T., III *J. Phys. Chem. B* **2006**, *110*, 20872.
- (64) Ramakrishna, G.; Goodson, T., III *J. Phys. Chem. A* **2007**, *111*, 993.
- (65) Ramakrishna, G.; Bhaskar, A.; Bauerle, P.; Goodson, T., III *J. Phys. Chem. A* **2008**, *112*, 2018.
- (66) Varnavski, O. P.; Xan, X.; Mongin, O.; Blanchard-Desce, M.; Goodson, T., III *J. Phys. Chem. C* **2007**, *111*, 149.
- (67) Bhaskar, A.; Ramakrishna, G.; Hagedorn, K.; Varnavski, O.; Osteritz, E. M.; Bauerle, P.; Goodson, T., III *J. Phys. Chem. B* **2007**, *111*, 946.
- (68) Williams-Harry, M.; Bhaskar, A.; Ramakrishna, G.; Goodson, T., III; Imamura, M.; Matawari, A.; Nakao, K.; Enozawa, H.; Nishinaga, T.; Iyoda, M. *J. Am. Chem. Soc.* **2008**, *130*, 3252.

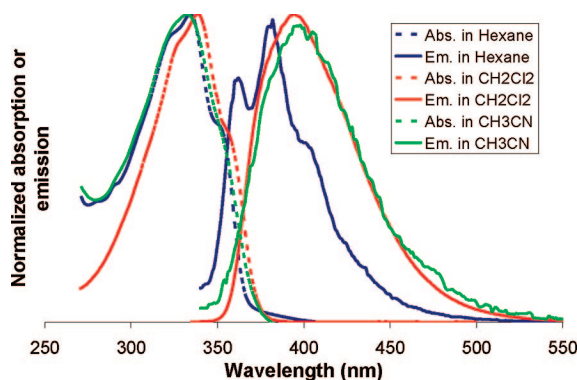


Figure 16. UV-vis and emission data for MeVinylStilbeneOS in three solvents.

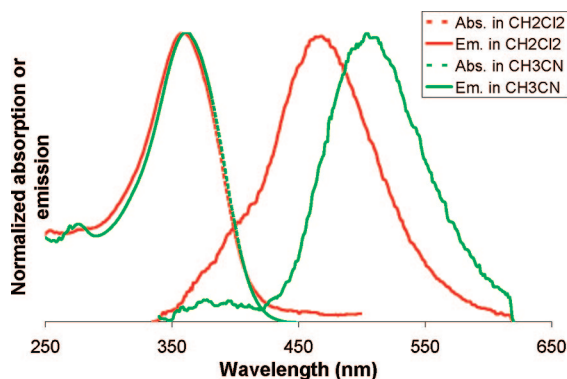


Figure 17. UV-vis and emission data for NH₂VinylStilbeneOS in two good solvents.

of solvent polarity on its emission behavior. Figure 16 provides UV-vis and emission data for MeVinylStilbeneOS in several solvents while Figure 17 records the same type of data for NH₂VinylStilbeneOS. What is immediately apparent is that while the red-shifts seen for MeVinylStilbeneOS are modest with changes in solvent polarity, those of NH₂VinylStilbeneOS are quite large by comparison. The extent of the shift is more impressive when considered against the shifts of all of these molecules as a function of solvent polarity. A search of the literature provides a better perspective of the degree of shift observed. Table 5 lists sets of representative organic molecule UV-vis and emission properties as a function of solvent and type of substitution.

The simplest member of this system, stilbene, absorbs (CH₃CN) at 307 nm and emits at 350 nm. The addition of a *p*-vinyl group shifts these values to 325 and 369 nm in the same solvent. Attaching it to the silsesquioxane cage leads to a red-shift (331 and 388 nm) of less than 10 nm in the same solvent. The addition of a *p*-CH₃ causes a nominal UV-vis red-shift of 20 nm from the parent silsesquioxane in emission, to 398 nm with essentially no change in luminescence quantum efficiencies. However the addition of a *p*-CH₃O group shifts the UV-vis about 10 nm from the

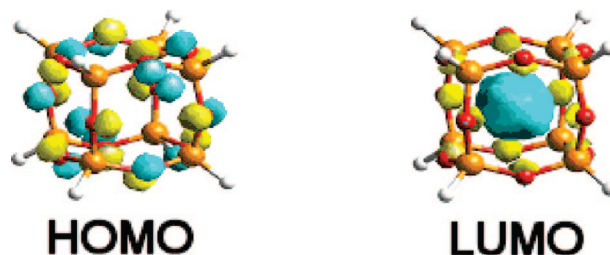


Figure 18. (a) HOMO and (b) LUMO of [XSiO_{1.5}]₈.⁷⁷

parent silsesquioxane but results in a 40 nm red-shift in the emission maximum to 430 nm. Most surprising of all is that addition of a *p*-NH₂ red-shifts the UV-vis by 30 nm from the parent silsesquioxane *but shifts the emission by 120 nm from the parent in the same solvent*.

If we now consider the effect of adding a *N,N'*-dimethylamino pendant to the parent stilbene, the UV-vis maximum is red-shifted 40 nm and the emission 90 nm in the same solvent. Thus we see that the UV-vis red-shift in NH₂VinylStilbeneOS is smaller than *N,N'*-dimethylaminostilbeneOS and yet the emission shift is 30 nm greater. One might argue that this is a consequence of the slightly longer conjugation length of NH₂VinylStilbeneOS, but this should be reflected in both ground and excited states relatively equally. That is, the ground-state of NH₂VinylStilbeneOS could be expected to shift at least as much as seen for the *N,N'*-dimethylaminostilbeneOS.

There is another explanation that may better describe this enormous shift. There have now been more than seven modeling studies of [RSiO_{1.5}]₈ (R = H, F, HO, NH₂ alkyl, etc.) done by multiple groups.^{73–78} The majority of these studies find that the [RSiO_{1.5}]₈ HOMO involves the 2p lone pair states of A_{2g} symmetry on the oxygen atoms, Figure 18a. Likewise they also find that the LUMO has 4A₁ symmetry and involves contributions from all Si, oxygen atoms, and the organic substituents, is spherical, and resides in the core center, Figure 18b.^{73,78} This “core” state is highly electrophilic and may influence emission behavior.

Indeed, Bassindale et al.^{79,80} recently synthesized silsesquioxanes with encapsulated F[–] and suggest that their stability may be enhanced by interaction with a low lying LUMO within the core suggesting that the idea is not novel to us and further supporting our proposed explanation. In contrast, Pach and Stosser⁸¹ recently studied and modeled the behavior of H⁺ and D⁺ in [HSiO_{1.5}]₈ and [MeSiO_{1.5}]₈

(69) Varnavski, O. P.; Ranasinghe, M. I.; Yan, X.; Bauer, C. A.; Chuang, S.-J.; Perry, J. W.; Marder, S. R.; Goodson, T., III *J. Am. Chem. Soc.* **2006**, *128*, 10988.

(70) Samori, S.; Hara, M.; Tojo, S.; Fujitsuka, M.; Majima, T. *J. Photochem. Photobiol., A* **2006**, *179*, 115.

(71) Letard, J.-F.; Lapouyade, R.; Rettig, W. *J. Am. Chem. Soc.* **1995**, *115*, 2441.

(72) Measured in this work.

(73) (a) Ossadnik, C.; Veprek, S.; Marsmann, H. C.; Rikowski, E. *Monat. Chem.* **1999**, *130*, 55. (b) Schneider, K. S.; Zhang, Z.; Banaszak-Holl, M. M.; Orr, B. G.; Pernisz, U. C. *Phys. Rev. Lett.* **2000**, *85*, 602.

(74) (a) Ossadnik, C.; Veprek, S.; Marsmann, H. C.; Rikowski, E. *Monatsh. Chem.* **1999**, *130*, 55. (b) Azinovic, D.; Cai, J.; Eggs, C.; Konig, H.; Marsmann, H. C.; Veprek, S. *J. Lumin.* **2002**, *97*, 40.

(75) Anderson, S. E.; Bodzin, D. J.; Haddad, T. S.; Boatz, J. A.; Mabry, J. M.; Mitchell, C.; Bowers, M. T. *Chem. Mater.* **2008**, in press.

(76) (a) Xiang, K.-H.; Pandey, R.; Pernisz, U. C.; Freeman, C. *J. Phys. Chem. B* **1998**, *102*, 8704. (b) Cheng, W.-D.; Xiang, K.-H.; Pandey, R.; Pernisz, U. C. *J. Phys. Chem. B* **2000**, *104*, 6737.

(77) Lin, T.; He, C.; Xiao, Y. *J. Phys. Chem. B* **2003**, *107*, 13788.

(78) Neurock, M.; Filhol, J.-S.; Lee, C.-Y. Unpublished work.

(79) Bassindale, A. R.; Pourny, M.; Taylor, P. G.; Hursthouse, M. B.; Light, M. E. *Angew. Chem., Int. Ed.* **2003**, *42*, 3488.

(80) Bassindale, A. R.; Parker, D. J.; Pourny, M.; Taylor, P. G.; Horton, P. N.; Hursthouse, M. B. *Organometallics* **2004**, *23*, 4400.

(81) Pach, M.; Stosser, R. *J. Phys. Chem. A* **1997**, *101*, 8360.

cages. They find that "...H is more stable outside the cage", indirectly agreeing with Bassindale and with previous theoretical findings that the interior is electrophilic.

Consequently, one possible interpretation would be that this highly electrophilic LUMO acts as a strong acceptor for the CT electron from the amine group. This leads to several interesting but at present speculative conclusions. First, the cage core is actually able to interact electronically with the conjugated vinyl stilbene and can no longer be considered as a classical insulating silica cage. Second, if the LUMO is indeed 3-D, then all eight vinylstilbenes may interact simultaneously setting the stage for some form of 3-D electronic interactions. Efforts to develop 3-D luminescent molecules have been discussed in the literature recently.^{82–85}

We are currently pursuing this idea in more detail using stilbene cage systems synthesized as recently described⁹ and will be reporting on related systems shortly.⁸⁶

-
- (82) Ganesan, P.; Yang, X.; Loos, J.; Savenije, T. J.; Abellon, R. D.; Zuilhof, H.; Sudholter, E. R. R. *J. Am. Chem. Soc.* **2005**, *127*, 14530.
(83) Oldham, Jr., W. J.; Lachicotte, R. J.; Bazan, G. C. *J. Am. Chem. Soc.* **1998**, *120*, 2987.
(84) Robello, D. R.; Andre, A.; McCovick, T. A.; Kraus, A.; Mourey, T. H. *Macromolecules* **2002**, *35*, 9334.
(85) Wang, S.; Oldham, W. J., Jr.; Hudack, Jr., R. A.; Bazan, G. C. *J. Am. Chem. Soc.* **2000**, *122*, 5695.
(86) Neurock, M.; Filhol, J.-S.; Lee, C.-Y.; Laine, R. M.; Brick, C. M.; Roll, M.; Sulaiman, S. Unpublished work.

Conclusions

The current work suggests that cubic silsesquioxanes offer unique opportunities to build new types of 3-D molecular structures around a nanometer size octafunctional core with cubic symmetry. The chemistries explored here were meant only to be representative of the many diverse simple and complex molecular structures that can be created using these simple cages as a basic starting point. It is also clear that these compounds offer unique properties in their own rights as witnessed by the novel luminescence properties that may suggest 3-D conjugation in the excited state and in the formulation of nanocomposites with important new properties as evidenced by the polymerized styrenyl cage materials.

Acknowledgment. We would like to thank Delphi, Nippon Shokubai Ltd., Canon Ltd., Mayaterials Inc., and especially NSF for funds through Grant CGE 0740108. S.S. would like to thank Dr. Scott Woehler for the assistance in obtaining ²⁹Si NMR spectra. The two-photon cross-section and steady state photonic properties measured by A.B., J.Z., R.G., and T.G. were supported by a grant from NSF Polymer Division.

Supporting Information Available: Tables with NMR data, MALDI-ToF spectra, and plot of the two photon cross-section (PDF). This material is available free of charge via the Internet at <http://pubs.acs.org>.

CM801017E